# Interchannel interaction versus relativistic effects: Xe 5*p* photoionization revisited

B. Zimmermann,[1] G. Snell,[2] B. Schmidtke,[2] J. Viefhaus,[1] N. A. Cherepkov,[3] B. Langer,[1,4] M. Drescher,[2] N. Müller,[2] U. Heinzmann,[2] and U. Becker[1]

[1]*Fritz-Haber-Institut der Max-Planck-Gesellschaft, Faradayweg 4-6, 14195 Berlin, Germany*

[2]*Fakultät für Physik, Universität Bielefeld, Universitätsstraße 25, 33615 Bielefeld, Germany*

[3]*State University of Aerospace Instrumentation, 190000 St. Petersburg, Russia*

[4]*Max-Born-Institut für Nichtlineare Optik und Kurzzeitspektroskopie, Max-Born-Straße 2A, 12489 Berlin, Germany*

(Received 29 June 2001; published 8 November 2001)

Xenon 5*p* subshell photoionization has been studied in the vicinity of the Xe 4*d* shape resonance by angle and spin resolved photoelectron spectroscopy. Dipole matrix elements and relative phase shifts derived from these experimental data are compared with calculations with regard to the strength of interchannel and relativistic interactions. The comparison shows strong influence of interchannel interactions on the transition-matrix elements, particularly on the phase shift in the vicinity of the 4*d* shape resonance, but gives little evidence for relativistic interactions of comparable strength.

DOI: 10.1103/PhysRevA.64.062501 PACS number(s): 32.80.Hd, 32.80.Fb

One of the most intriguing problems in atomic photoionization is how to represent the approximation of this fundamental process with a reasonable accuracy. There are three types of interactions where this question has to be raised: (1) the multipolarity of the interaction operator; (2) the extent to which interchannel and (3) relativistic interactions have to be taken into account. Ideally, one would like to be as rigorous as possible, but experiments do not generally provide enough information on the photoionization process to justify such a rigorous treatment. This means in a quantum-mechanical sense, that the number of independent transition-matrix elements is too high, as in practice there is no set of complementary experimental information available from which these matrix elements can be derived semi-empirically. This statement does not say anything about the principal existence of such a complete set of experimental data, it rather comments on the practical availability of such data sets. This is the reason why, in most photoionization studies, the first approximation made is the dipole approximation. This has been considered a good approximation roughly up to 1000 eV of photon energy. More recent studies have shown that nondipole effects may play a significant role at low kinetic energies under certain circumstances [1,2]. Being aware of this, it is still reasonable to apply the dipole approximation, because the impact of the different multipoles may be separated, both experimentally and theoretically, if the appropriate detection geometry is used. Since at present there are only very few theoretical treatments [3,4] available that would provide a quantum-mechanically complete description including nondipole effects, the first step to analyze the photoionization dynamics over large energy ranges is still the dipole approximation.

In this approximation there are two independent interactions, which play an important role in atomic photoionization: interchannel and relativistic interactions. Their effect on the description of photoionization is different. Interchannel interaction sometimes causes dramatic changes in the size of the photoionization parameters, however, it does not require a larger number of photoionization parameters. All changes resulting from this interaction are contained within the chosen set of parameters. In contrast, relativistic interactions force a different formulation of the process in terms of more independent parameters than used in a nonrelativistic description. This is due to the spin-orbit interaction, which causes relativistic effects in atomic photoionization. This interaction gives rise to a splitting of the subshell photoelectron lines into *j*-dependent components that must be treated independently. The number of independent photoionization parameters in a relativistic formulation is, even in the case of most closed-shell atoms, more than three times that used in a nonrelativistic formulation. Early studies of this problem concentrated on the xenon 5*s* and 5*p* subshell photoionization. In case of the Xe 5*s* subshell, the situation concerning the importance of relativistic effects was particularly easy to analyze because of the emission of either one partial wave $(\epsilon p)$ in the nonrelativistic case or two partial waves $(\epsilon p_{1/2}, \epsilon p_{3/2})$ in the relativistic case. The relativistic description requires in its simplest case a pronounced deviation of the angular-distribution-anisotropy parameter $\beta$ from its nonrelativistic fixed value of 2 in the presence of a Cooper minimum. This prediction, its first experimental verification, later revision and the difficult way to the final settlement of this issue caused a longstanding interest on the interplay between interchannel coupling and relativistic interactions [5]. The exploraton of this problem for subshells with $l>0$ is even more complex and here the Xe 5*p* subshell becomes a show case example because it is subject to pronounced interchannel interactions, particularly with the predominant 4*d* subshell, with large spin-orbit splitting, pointing to strong relativistic interactions. For a long time, only two photoionization parameters were accessible to experimental verification: the partial cross section $\sigma$ and the electron-angular-distribution-asymmetry parameter $\beta$. These two parameters generally do not provide enough information for a complete photoionization experiment, even in a nonrelativistic description. Nevertheless, a sensitive comparison between selected experimental and theoretical data provided first insight into the relevance of both interchannel and relativistic interaction already at a very early stage of photoionization studies [6,7] The conclusion of these studies was that both relativistic and

 

interchannel effects are relevant, however, quantifying these effects was difficult on the basis of the available data. Only recent studies [8] suggested that in resonant photoemission both interactions are of the same magnitude.

More highly differentiated measurements, such as the spin-sensitive detection of the photoelectron opened the door to a really complete photoionization experiment [9,10]. Here, xenon subshell photoionization served as a benchmark experiment [11]. A critical reanalysis of these data and their interpretation was, however, surprising: The set of independent photoionization measurements was not really independent [12]. Within a certain range of values of the measurements they appeared to depend on each other making it impossible to derive the number of parameters necessary in a relativistic formulation. Fortunately, the reanalysis revealed a negligible relativistic phase shift as being consistent with a reduced parameter model. This situation encouraged for spin-sensitive photoelectron measurements over an extended energy range, in particular, covering the region of strong interchannel interaction between the xenon $5p$ and $4d$ subshells. Such measurements could reveal the relative importance of relativistic vs interchannel interactions.

The corresponding experiments were performed at the synchrotron radiation facilities Hasylab at DESY (Hamburg) and BESSY (Berlin) using the undulator beam lines BW3 and U1/U2, respectively. The delivered photons were employed to ionize an effusive beam of xenon atoms. Two of the beamlines were constructed to produce highly linearly polarized radiation, while the third delivered circularly polarized light for a limited range of photon energies. For higher energies, a multilayer acting as a quarter-wave plate was used to convert linearly polarized light into circularly polarized light [13]. For all photon energies, we could thus determine both kinds of spin polarization of the electrons: $P_{trans}$—the transferred polarization from circularly polarized light to the emitted electron, and $P_{dyn}$—the so-called dynamical polarization being connected with an excitation by linearly polarized light [14]. In fact, both kinds of spin polarization have dynamical as well as transferred aspects concerning the mechanism of spin polarization via spin-orbit coupling, however, in case of circularly polarized light the direct polarization transfer is the dominating part whereas for linearly polarized light the magnitude of the produced alignment, another dynamical component of photoionization, plays an equally important role. The electron spin polarization was measured using a spherical Mott polarimeter in combination with a time-of-flight electron spectrometer. This experimental arragement has been used recently for the spin-polarization measurements of photoelectrons and Auger electrons emitted during Xe $3d$ and $4d$ photoionization [15–17]. Details of this setup are given in these references. Here, we concentrate only on the results and their discussion.

Figure 1 shows the results of all the experiments in an overview together with the older cross section and the angular-distribution data compared with relativistic and nonrelativistic theoretical calculations. Due to the limited range of photon energies for circularly polarized light, there are less data points shown for the transferred spin polarization

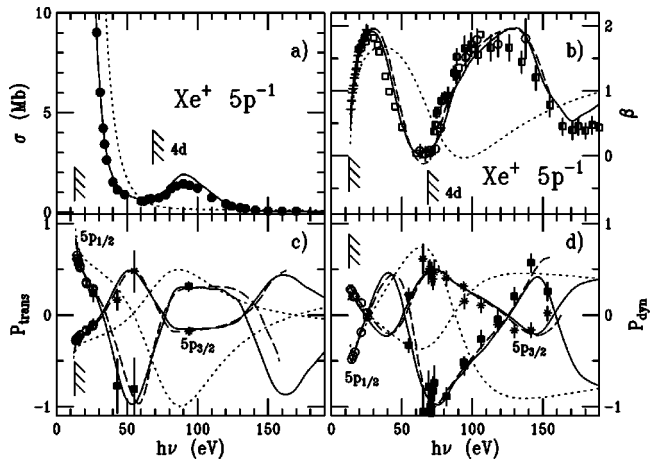


FIG. 1. Parameter of Xe $5p$ photoionization: (a) cross section $\sigma$: (●) [18]; (b) anisotropy parameter $\beta$: (+) [19], (□) [7], (half filled □) [20], (○) [21]; (c) transferred and (d) dynamical spin polarization (see [16]): (○) [11,22], ($5p_{1/2}$:■, $5p_{3/2}$:*)—present measurements. (The region between 65 eV and 70 eV is effected by autoionizing resonances.) The dashed lines are relativistic RRPA [23]. The solid lines represent the nonrelativistic RPAE calculation and the dotted lines the nonrelativistic HF calculation (both using [24]).

than for the dynamical spin polarization. For completeness we also show the low-energy data points of Heckenkamp *et al.* [11].

The strong modulation of both types of spin polarization predicted by theory is well corroborated by our measurements. As we will show later, the driving force behind this oscillatory behavior is the phase shift between the $\varepsilon s$ and $\varepsilon d$ partial waves. Here, we will first concentrate on the difference between the relativistic and the nonrelativistic theoretical predictions in the context of the new experimental results. In order to make the two sets of theoretical curves comparable, we had to perform nonrelativistic calculations within the random-phase-approximation with exchange (RPAE) [25]. These calculations made it not only possible to show improved curves for the transferred and dynamical spin polarization, but also to extract the corresponding dipole matrix elements with relative phase shifts in order to visualize the dynamical behavior of the interchannel interaction. Comparing the relativistic random-phase approximation (RRPA) with the nonrelativistic (RPAE) results shows at a glance that the differences are negligible near threshold where the former measurements were taken [26], and gain some measurable size only in the wings of the minimum around 50 eV or following maximum. This is due to the fact that the positions of these extremes are measurably affected by the relativistic interactions. Unfortunately, there are not too many experimental points in this energy interval, and their errors are still relatively large. Nevertheless, there are three data points that distinguish between the two kinds of calculations: the $5p_{1/2}$ transferred polarization at 43 eV and the corresponding dynamical polarization at 53 eV and 140 eV. The first two data points favor the nonrelativistic, while the last favors the relativistic calculation, although this agreement is counterbalanced by the following data point at 150 eV. Tak-

ing this together, there is a slight preference for the nonrelativistic calculation. One has, however, to keep in mind that there is a marginal difference between the two approaches in the whole energy region investigated pointing to small relativistic interactions.

This weak impact of the relativistic interactions makes it possible to describe the photoionization dynamics of the xenon $5p$ subshell photoionization approximately in terms of a nonrelativistic three-parameter model. The only extension of this model is concerned with the spin-orbit branching ratio of the $5p_{3/2}$ and $5p_{1/2}$ components, which is sensitive to the coupling properties of the ionic core rather than the continuum electron. The effect of the spin-orbit branching ratio, however, can in practice be included as a correction in the $LS$-based three-parameter model and so does not significantly affect the complexity of the calculation, similarly to $4d_{5/2}$ and $4d_{3/2}$ spin-orbit components in the Xe $4d$ photoionization [16].

Following the theoretical arguments that the $LS$-coupling-based three-parameter model is a good approximation for the Xe $5p$ subshell photoionization, we are able to derive the $R_s$ and $R_d$ dipole matrix elements along with the relative phase shift between the corresponding partial waves of the emitted photoelectron from the experimental data. Thus, semi-expirically determined matrix elements [27] and phase shifts may be compared with calculated matrix elements and phases, with or without electron correlation, using either the Hartree-Fock (HF) method or the RPAE. Figure 2 shows the ratio of the two radial matrix elments $\gamma = R_d/R_s$ and the relative phase $\Delta$ between them for both calculations in a two and three dimensional representation. This representation shows the whole dynamical evolution of the Xe $5p$ photoionization process within a particular model, exhibiting the differences between the RPAE and HF model very clearly. The HF curve is characterized by making one turn in the complex plane from threshold to the asymptotic limit, thereby crossing the zero point of this plane at the Cooper minimum position. In contrast to this relatively simple behavior, RPAE also accounts for interchannel interactions that transforms this evolution curve into a spiral with several turns and more importantly no zero crossing at the energy position of the Cooper minimum. This behavior has consequences for the description of the photoionization process in terms of the usual representation of matrix elements and phases as shown in Fig. 3. Figure 3(a) shows the relative phase shift and Fig. 3(b) displays the radial parts of the two dipole matrix elements. The agreement between the semiempirically derived data and the RPAE calculation is excellent and illustrates the validity of the chosen model for the description of the Xe $5p$ photoionization. The interchannel interaction between the $4d$ and $5p$ subshells acts basically on the $\varepsilon d$ partial wave, shifting the zero crossing (the Cooper minimum) to lower photon energies and leading to the pronounced maximum in the $R_l^2$-related $5p$ partial cross section. Note that according to Fig. 2 the RPAE results do not show a zero crossing but instead a phase jump of $\pi$, smoothed due to the interaction between the two channels. In order to adjust the asymptotic behavior of the RPAE calculation to the HF results we have removed the phase jump by changing the sign in the corresponding matrix elements.

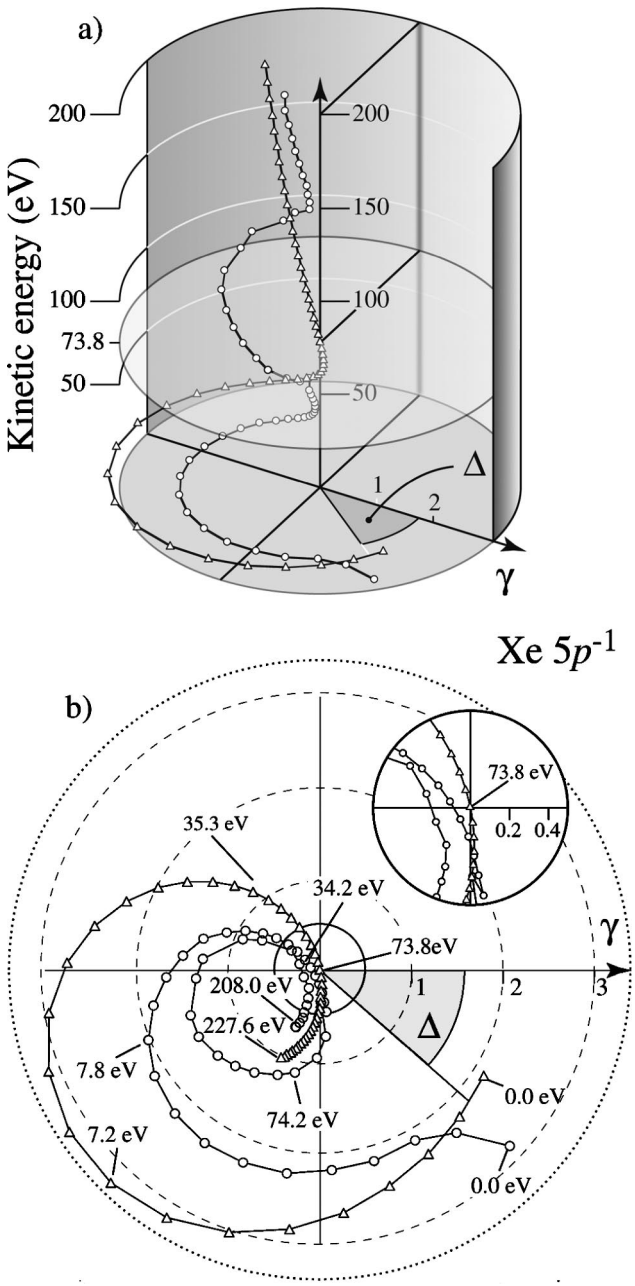


FIG. 2. Ratio $\gamma$ of the two radial matrix elements $R_d$ and $R_s$ and their relative phase shift $\Delta$ obtained by either the HF ($\triangle$) or RPAE ($\bigcirc$) method. The corresponding curves over kinetic energy are shown (a) in a three-dimesional representation in cylindrical coordinates and (b) in form of a projection onto the bottom plane with an enlargement of the region around zero.

More interesting than this effect is the behavior of the relative phase shift, which would drop quickly from threshold then maintain a slow decrease with photon energy if interchannel interactions were not present. The HF phase shift exactly represents this behavior. In contrast, the measured phase shift starts to drop more steeply at the $4d$ threshold reaching a minimum of $\approx -\pi$ lower phase shift value 40 eV above the $4d$ shape resonance maximum before returning

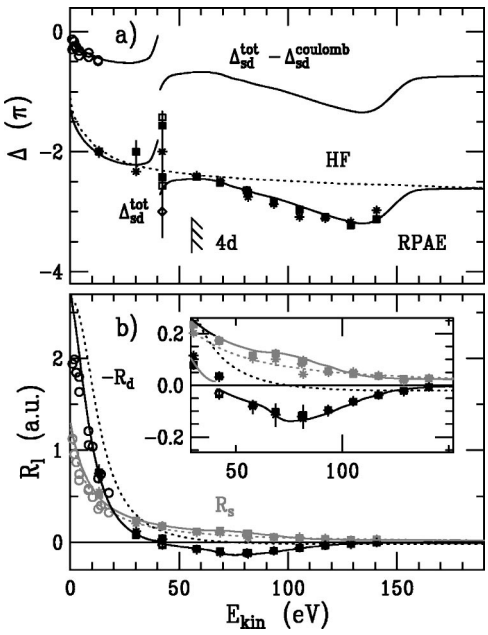


FIG. 3. Phase shifts (a) and matrix elements (b) of Xe $5p$ photoionization: (○) former data from Refs. [11,12,22], ($5p_{1/2}$:■,□;$5p_{3/2}$:*, ◇)—present results. □ and ◇ represent further solutions from a sign change of $R_d$ and a phase shift by $\pi$. The solid line is the result of the present RPAE calculation, whereas the dotted line represents the HF calculation (both using [24]). The discontinuity in the RPAE curves is due to the chosen representation (see text).

to the HF value.

This dramatic phase change is the result of the strong interaction between the two partial waves in the vicinity of the $4d$ shape resonance, driving the two partial waves spatially further apart than in the noninteracting case. This is a very direct consequence of the physical process that causes the strong interchannel interaction, namely, the fact that the $4d$ subshell becomes highly polarized when losing one electron. The resulting field distortion around the $4d$ shell is not only sufficient to drive the emission of electrons from the $5s$ and $5p$ subshells but also to distort the internal coherence properties of the corresponding $l$-dependent partial photoelectron waves. This phase-shift variation quantitatively describes the observed strong oscillations in all phase-shift dependent photoionization quantities such as angular distribution and spin polarization in Fig. 1.

One may consider this behavior as the effect of a continuum resonance on another continuum channel. Since there is a resonant character involved in this present example one might expect to see a stronger influence of relativistic interactions similar to those observed for certain discrete resonances in the continuum of an open photoionization channel [8,28]. But this is obviously not the case. The reason for the unexpected simpler behavior is the continuum character of the $4d$ shape or giant resonance, which is built upon the $LS$-coupled $\varepsilon s$, $\varepsilon d$ continuum waves of the emitted $4d$ photoelectron where the core hole is considered to be coupled in the $jj$-coupling scheme but the ejected electron couples its spin and angular momentum to this state following the $LS$ coupling rules. The $j$ of the final ionic state couples with the angular momentum $l$ of the photoelectron first to an angular momentum $k$ before the spin of the photoelectron is further coupled to the angular momentum of the complete ion-electron system. Because the validity of this $jk$-coupling scheme increaes with increasing principal quantum number $n$ [29], it is reasonable to assume that the $jk$-coupling scheme is also valid above threshold to a certain extent. This is in marked contrast to the findings for resonant photoionization where the excitation of certain resonances with distinct $j$ values undermines the validity of this scheme due to $j$-selective autoionization. This assumption makes the approximate treatment of nonresonant photoionization feasible with respect to a complete description, even in cases where the number and experimental uncertainty of available independent measurements is not sufficient for a rigorous relativistic treatment [30].

In summary, new measurements and calculations of the transferred and dynamical spin polarization of the Xe $5p$ photoelectrons in the vicinity of the $4d$ shape resonance revealed strong interchannel interactions with particular effect on the relative phase shift between the two outgoing partial photoelectron waves. There is, however, little evidence for the presence of strong relativistic effects in the continuum. This unbalanced weighting of two in resonant photoionization equally strong interactions is explained by the approximate $LS$ coupling of the $4d$ photoelectron to the ionic core still in the presence of a shape resonance.

N.A.C. acknowledges financial support from the Fritz-Haber-Institut der MPG, Berlin, granted to him during the work on this paper.

[1] B. Krässig, M. Jung, D.S. Gemmell, E.P. Kanter, T. LeBrun, S.H. Southworth, and L. Young, Phys. Rev. Lett. **75**, 4736 (1995).
[2] O. Hemmers, G. Fisher, P. Glans, D.L. Hansen, H. Wang, S.B. Whitfield, R. Wehlitz, J.C. Levin, I.A. Sellin, R.C.C. Perera, E.W.B. Dias, H.S. Chakraborty, P.C. Deshmukh, S.T. Manson, and D.W. Lindle, J. Phys. B **30**, L727 (1997).
[3] J.W. Cooper, Phys. Rev. A **47**, 1841 (1993).
[4] A. Bechler and R.H. Pratt, J. Phys. B **32**, 2889 (1999).
[5] For a review see: A.F. Starace and S.T. Manson, in *VUV and Soft X-Ray Photoionization*, edited by U. Becker and D.A. Shirley (Plenum Press, New York, 1996), p. 81.
[6] W.R. Johnson and K.T. Cheng, Phys. Rev. A **20**, 978 (1979).
[7] M.O. Krause, T.A. Carlson, and P.R. Woodruff, Phys. Rev. A **24**, 1374 (1981).
[8] O. Yenen, K.W. McLaughlin, D.H. Jaecks, M.M. Sant'Anna, and E.A. Seddon, Phys. Rev. Lett. **86**, 979 (2001).
[9] For a review see: U. Heinzmann and N.A. Cherepkov, in *VUV*

*and Soft X-Ray Photoionization*, edited by U. Becker and D.A. Shirley (Plenum Press, New York, 1996), p. 521.

[10] J. Kessler, *Polarized Electrons*, 2nd ed. (Springer, Berlin, 1985).

[11] C. Heckenkamp, F. Schäfers, G. Schönhense, and U. Heinzmann, Z. Phys. D: At., Mol. Clusters **2**, 257 (1986).

[12] B. Schmidtke, M. Drescher, N.A. Cherepkov, and U. Heinzmann, J. Phys. B **33**, 2451 (2000).

[13] J. Viefhaus, L. Avaldi, G. Snell, M. Wiedenhöft, R. Hentges, A. Rüdel, F. Schäfers, D. Menke, U. Heinzmann, A. Engelns, J. Berakdar, H. Klar, and U. Becker, Phys. Rev. Lett. **77**, 3975 (1996).

[14] H. Klar, J. Phys. B **13**, 4741 (1980).

[15] G. Snell, M. Drescher, N. Müller, U. Heinzmann, U. Hergenhahn, J. Viefhaus, F. Heiser, U. Becker, and N.B. Brookes, Phys. Rev. Lett. **76**, 3923 (1996).

[16] G. Snell, B. Langer, M. Drescher, N. Müller, B. Zimmermann, U. Hergenhahn, J. Viefhaus, U. Heinzmann, and U. Becker, Phys. Rev. Lett. **82**, 2480 (1999).

[17] G. Snell, U. Hergenhahn, N. Müller, M. Drescher, J. Viefhaus, U. Becker, and U. Heinzmann, Phys. Rev. A **63**, 32 712 (2001).

[18] U. Becker, D. Szostak, H.G. Kerkhoff, M. Kupsch, B. Langer, R. Wehlitz, A. Yagishita, and T. Hayaishi, Phys. Rev. A **39**, 3902 (1989).

[19] S.H. Southworth, A.C. Parr, J.E. Hardis, J.L. Dehmer, and D.M.P. Holland, Nucl. Instrum. Methods Phys. Res. A **246**, 782 (1986).

[20] S. Southworth, U. Becker, C.M. Truesdale, P.H. Kobrin, D.W. Lindle, S. Owaki, and D.A. Shirley, Phys. Rev. A **28**, 261 (1983).

[21] L. Torop, J. Morton, and J.B. West, J. Phys. B **9**, 2035 (1976).

[22] U. Heinzmann, J. Phys. B **13**, 4353 (1980); **13**, 4367 (1980).

[23] K.N. Huang, W.R. Johnson, and K.T. Cheng, At. Data Nucl. Data Tables **26**, 33 (1981).

[24] M.Ya. Amusia and L.V. Chernysheva, *Computation of Atomic Processes—A Handbook for the ATOM Programs* (Institute of Physics Publishing, Bristol, 1997).

[25] N.A. Cherepkov, J. Phys. B **12**, 1279 (1979).

[26] N.A. Cherepkov, J. Phys. B **13**, L689 (1980).

[27] The relations between $\sigma$, $\beta$, $P_{dyn}(E_{kin})$, $P_{trans}(E_{kin})$, $R_s$, $R_d$, and $\Delta_{sd}$ are expressed as

$$\sigma = 4\pi^2 \alpha h\nu \tfrac{2}{3}(R_s^2 + 2R_d^2),$$

$$\beta = [2R_d^2 - 4R_s R_d \cos(\Delta_{sd})]/(R_s^2 + 2R_d^2),$$

$$P_{dyn1/2} = [6 R_s R_d \sin(\Delta_{sd})]/[2R_s^2 - 2R_s R_d \cos(\Delta_{sd}) + 5R_d^2] = -2 P_{dyn\,3/2},$$

$$P_{trans\,1/2} = [-2R_s^2 + 2R_s R_d \cos(\Delta_{sd}) + 4R_d^2]/[2R_s^2 - 2R_s R_d \times \cos(\Delta_{sd}) + 5R_d^2 = -2 P_{trans\,3/2}].$$

[28] A.A. Wills, T.W. Gorczyca, N. Berrah, B. Langer, Z. Felfli, E. Kukk, J.D. Bozek, and O. Nayandin, Phys. Rev. Lett. **80**, 5085 (1998).

[29] B. Langer, N. Berrah, A. Farhat, M. Humphrey, and D. Cubaynes, J. Phys. B **30**, 4255 (1997).

[30] T.W. Gorczyca, J.-E. Rubensson, C. Såthe, M. Ström, M. Agåker, D. Ding, S. Stranges, R. Richter, and M. Alagia, Phys. Rev. Lett. **85**, 1202 (2000).